

NEAR FLOOR AIR MOVEMENT IN AN ENCLOSURE WITH MIXING TYPE VENTILATION

Yuzhou Jin and John R. Ogilvie
University of Guelph
Guelph, ON, Canada

SUMMARY

The mean air velocity, and the RMS value, of the reverse flow in the zone up to 0.62 m above the floor of a 4.8 m (long) x 3.8 m (wide) x 3 m (high) building were measured with a hot-wire anemometer. The isothermal experiment was conducted for 35 inlet conditions in a full-scale slot-ventilated room. The vertical distributions of average time-mean velocity, RMS value, and turbulence intensity are shown at five horizontal positions along the flow direction at the floor. The mean velocity distributions at the mid floor region showed a similar form and approximated a jet profile. At the corners, the main rotary flow was deflected and the small recirculation flows were formed, causing high flow turbulence. Analysis of variance indicated that the same ventilation rates, arising from different combinations of inlet opening height and incoming air velocity, resulted in significantly different velocities in the measurement zone. The reverse flow velocities were not a function of ventilation flow rate alone.

THE J. C. ...
...

...

...

...

NEAR FLOOR AIR MOVEMENT IN AN ENCLOSURE WITH MIXING TYPE VENTILATION

Yuzhou Jin, John R. Ogilvie
University of Guelph
Guelph, ON, Canada

INTRODUCTION

Air drafts in the human or animal occupied zone due to inappropriate air velocity distribution may cause discomfort and complaint in ventilated or air-conditioned spaces. For example, Fanger et al. [1] showed that the percentage of dissatisfaction of persons exposed to the same mean air velocity was higher when flow turbulence intensity was high than when turbulence intensity was low. Air movement in an enclosure is a combined result of dynamic, thermal, climatic, mechanical and structural influences. No general methods or systems can be used to describe thoroughly this complicated process. Understanding on this issue is still inadequate.

Airflow patterns and airspeed in the occupied zone have been investigated by many researchers. Nielsen et al. [2] and Gosman et al. [3] used a small physical model to investigate two and three dimensional airflows. They found that air at the bottom of the model flowed in a direction opposite to that at the top where the jet was created, and called this reverse airflow or return flow. The maximum velocity in the reverse flow occurred close to the floor at a distance of $2/3$ room length from the supply opening. Nielsen [4] suggested a formula, with the same form as the equation for the centerline velocity of a plane wall jet and with an additional constant, to calculate the maximum velocity (U_m) in reverse flow. Skovgaard and Nielsen [5] used two simplified relationships for U_m i.e., $U_m \propto Q$ and $U_m \propto j^{0.5}$, where Q and j are the ventilation flow rate and the momentum flow through the inlet, respectively. Timmons et al. [6] and Timmons [7] also reported experiments on room airflow. Photographs and measurements showed that there was a threshold Reynolds number (Re) above which the flow patterns and dimensionless velocity became independent of changes in Re . The threshold Re was proportional to the physical dimension of model. Hanzawa et al. [8] and Melikov et al. [9, 10] investigated practical airflow characteristics in the occupied zone in spaces with mechanical ventilation, heated without mechanical ventilation, and with displacement ventilation. The main flow

characteristics, including mean air velocity, turbulence intensity and their distributions, spectra of the turbulent kinetic energy, and length scales of turbulence, were reported.

Recently, the inlet jet momentum number J as an index of airflow patterns and airspeeds in the occupied zone has been reported [11]. The dimensionless jet momentum number is defined as $J = (QU_0)/(gV)$, where Q and U_0 are respectively ventilation flow rate and incoming jet air speed through the inlet; g is the acceleration of gravity; and V is the interior space volume. Ogilvie and Barber [11] reported linear relationships between floor air speeds and J . Spidler et al. [12] found that not only bulk air velocity but also the convective heat transfer coefficient in the room was proportional to the square root of the incoming J . Jin and Ogilvie [13] examined the individual effect of incoming air velocity and inlet slot height, and established equations for floor mean velocity and the RMS value of turbulent fluctuation with J .

Many of the early measurements were conducted in small-scale physical models. It is very difficult or impossible to reproduce certain practical flow phenomena by such reduced size models. Some results and conclusions lack complete, detailed and accurate information and, hence, were questionable. Limited experimental trials or tests may not dig out the real flow information, and may even misinterpret it. To understand the true flow characteristics, a comprehensive as well as an accurate experiment is essential.

The purpose of this study was to determine the air velocity distribution in reverse airflow in a full-scale ventilated enclosure. Slotted inlet and outlet openings were used. The interior airflow was assumed to be two-dimensional (based on the length to width/height ratio of the enclosure), and steady state. The measurements were conducted in isothermal and steady-state conditions and only when the full rotary flow pattern was established [13]. The range of flow rates was 7.5 to 60 air exchanges per hour (ACH) commonly used for industrial and agricultural ventilation air loading rates.

EXPERIMENTAL APPARATUS AND PROCEDURE

The experiment was conducted in an empty prototype building located at the University of Guelph, Ontario, Canada (Figure 1), to simulate a room 4.8 m long (L), 3.8 m wide (W) and 3 m high (H). An adjustable slot inlet and 0.1 m slot outlet extended the full width of the room (3.8 m). The room was ventilated by suction fans which could achieve ventilation flow rates up to 60 ACH by adjusting a vent on the fan box, the speed of the fan or combination of the above. Air was ejected and exhausted evenly through the slot planes and two-dimensional flow was ensured.

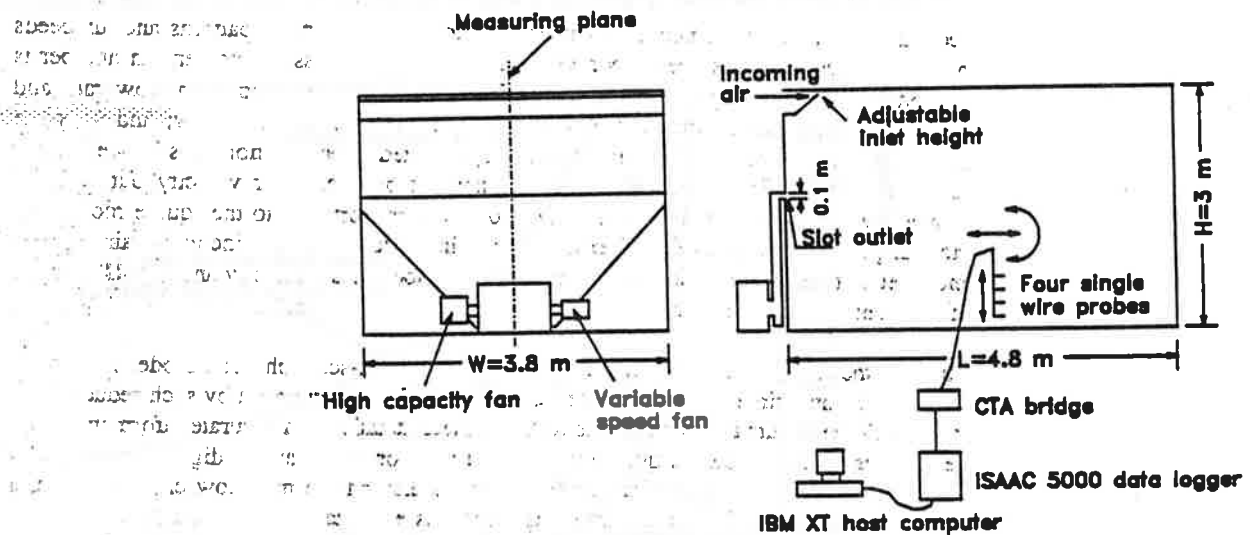


Fig. 1 Dimensions and geometries of the experimental enclosure and apparatus.

Velocity was measured by a hot-wire anemometer. Four single hot-wire probes (Dantec, model 55P11) were mounted in a rack on a testing rig, movable in both horizontal and vertical directions. Velocity was sampled at 100 Hz over a period of 30 seconds as suggested by Jin [15]. A mean and a root-mean-square (RMS) value, obtained from these 3,000 data (100 Hz x 30 s), were used to evaluate velocity characteristics for one measuring position since the steady-state air velocity was close to a Normal or Gaussian distribution [15].

A separate hot-wire probe was mounted in the centre of the slot to determine the incoming jet air speed. All data were sampled by a high speed analog-to-digital data logger (ISAAC 5000, Cyborg) controlled by a host computer (IBM XT). Hot-wire probe calibration was achieved by two devices, a rotating device and a wind tunnel for the calibration speed ranges from 0.1 to 1.0 m/s and from 1.0 to 15 m/s, respectively. Any effect due to temperature difference between calibration and measurement was corrected. Details about hot-wire calibration are given in Jin [15].

When the flows became fully rotary in the enclosure, the reverse flow velocity at the floor level was measured according to the 41 combinations (35 inlet configurations plus 6 replicates) of inlet velocity and inlet height shown on an airflow rate plan (Figure 2) and discussed in Jin and Ogilvie [13]. In the floor region, measurements were taken every 0.2L

(0.96 m) horizontally, and every 0.04 m vertically with the first point at 0.02 m and the last at 0.62 m above the floor (Figure 3), a total of 80 points for each of the inlet conditions.

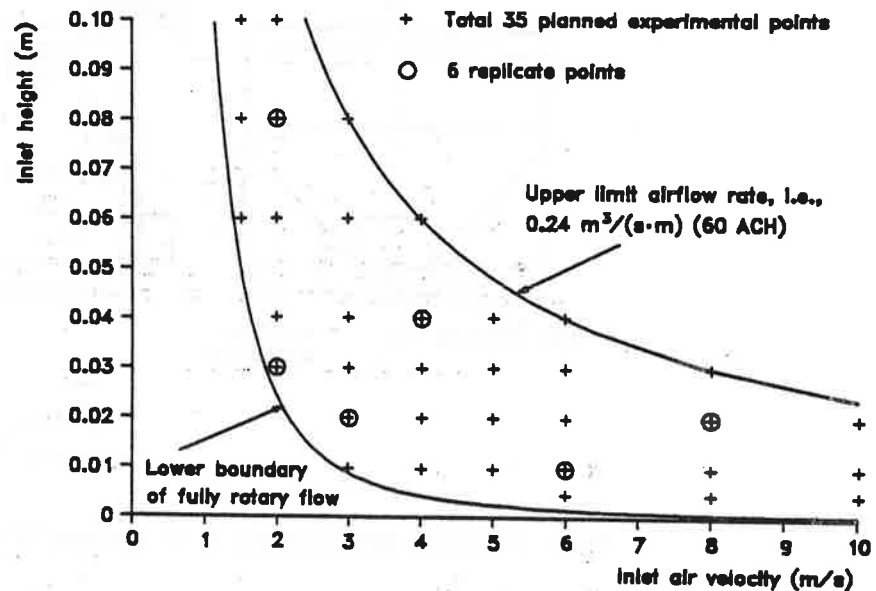


Fig. 2 Planned experimental and replication points between lower boundary of full rotary flow and upper limit flow rate on the airflow rate plan.

RESULTS AND DISCUSSION

Mean Velocity Distribution in Reverse Flow

To get an overall view of the flow at the floor region, the mean velocity was averaged over the 41 inlet conditions. Figures 4 and 5 show the non-normalized and normalized mean velocity distributions (solid lines) at 5 horizontal positions along the room length, respectively. The non-normalized velocity profiles were obtained by taking an average on the measured velocities from the 41 inlet conditions for each of the 80 floor positions. The normalized velocity profiles were obtained by dividing the floor velocity by the inlet velocity and then taking the average. To examine the individual velocity distribution, the profiles at two typical inlet conditions with the same ventilation flow rate (50 ACH) are shown on Figures 4 and 5.

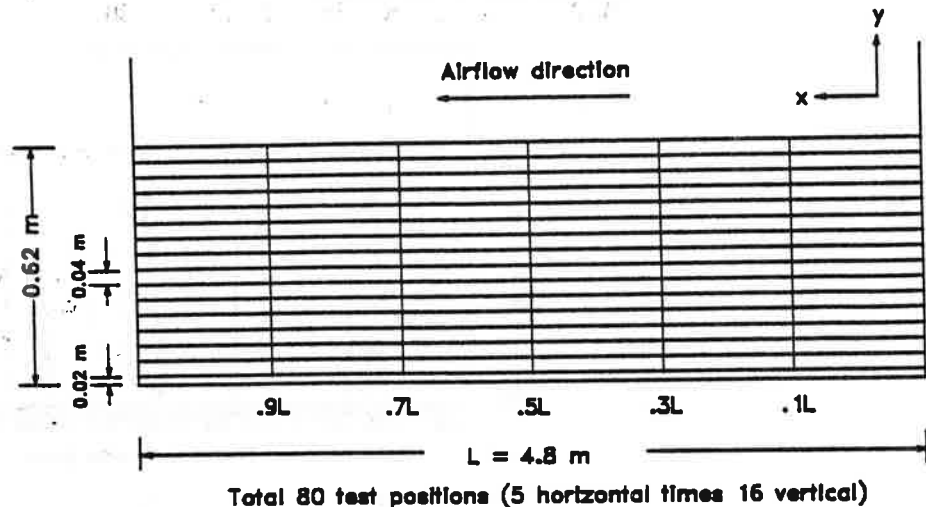


Fig. 3 Dimensions and geometries of velocity measuring positions at the floor region.

There were no differences in variations of flow distribution between non-normalized and normalized velocities, except for different scales. For the same ventilation flow rate through the inlet, velocity magnitudes were quite different for the two inlet conditions ($U_0 = 10$ m/s and $d = 0.02$ m vs. $U_0 = 2$ m/s and $d = 0.1$ m). The non-normalized reverse flow velocities of $U_0 = 10$ m/s and $d = 0.02$ m were much higher than those of $U_0 = 2$ m/s and $d = 0.1$ m (Figure 4). However, the situation was reversed when the velocity was normalized on the inlet velocity, i.e., the normalized velocities of $U_0 = 10$ m/s and $d = 0.02$ m were much smaller than those of $U_0 = 2$ m/s and $d = 0.1$ m (Figure 5). The high U_0 or high d resulted in high floor velocity. However, the influences of the two parameters were not equal. In other words, the floor velocities were different if one parameter was increased a certain amount and the other parameter was decreased in the same ratio, and *vice versa*.

As an example, analysis of variance was conducted on the floor mean velocity and the RMS value as affected by different U_0 and d combinations at the same Q of 15 and 40 ACH at which replicate measurements were performed (see Figure 2). Both mean velocity and the RMS value were different for different U_0 and d combinations at $Q = 15$ ACH ($P < 0.05$) and at $Q = 40$ ACH ($P < 0.01$). None of the replicate effects was significant at the 5% level [15]. As the result, the relationship $U_{rm} \propto Q$ suggested by Skovgaard and Nielsen [5] would no longer hold since the maximum velocity in the reverse flow U_{rm} , which is proportional to the averaged mean velocity over the entire occupied zone, is significantly different for the same Q . That is, the normalized reverse flow velocity is not a linear function of the inlet area. The equation $U_{rm} \propto j^{0.5}$ [5] may be a better form to express this relationship. The actual relationship $U_{rm} \propto j^{0.6}$ has been presented by Jin and Ogilvie [13] by correlating the

data from the 41 inlet conditions.

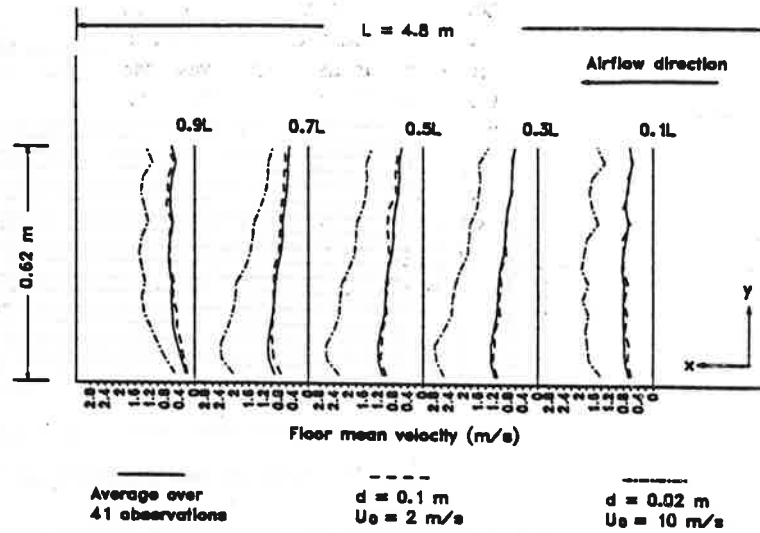


Fig. 4 The vertical distributions of non-normalized time-mean velocity at five floor positions for overall 41 inlet conditions and the two typical settings.

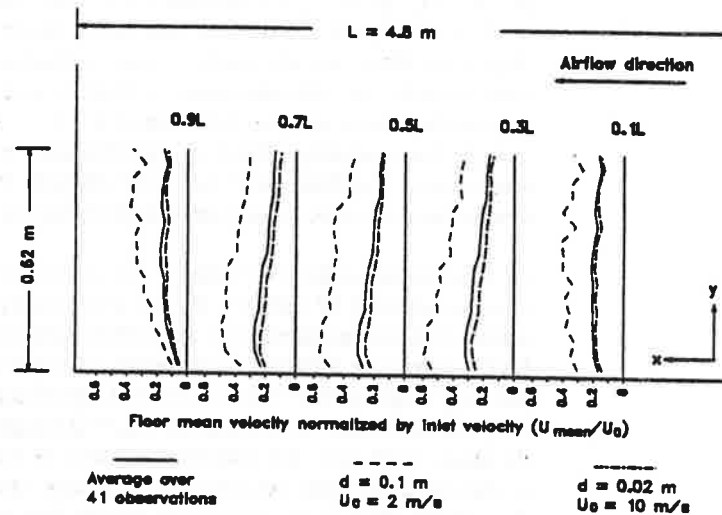


Fig. 5 The vertical distributions of normalized time-mean velocity at five floor positions for overall 41 inlet conditions and the two typical settings.

The mean airspeed distribution at three middle positions approximated a wall jet profile. For both scales, the maximum velocity occurred at the location $x = 0.3L$. Vertically, the speed increased to a maximum at about 0.1 m above the floor and then decreased, resembling a wall jet. A similar distribution was observed in the next two positions ($x = 0.5L$ and $0.7L$) down the flow, but the magnitude at each corresponding point was smaller due to the loss of kinetic energy as the flow went on. Figure 6 shows this decreasing trend of the normalized mean airspeeds averaged over different levels from the floor. Although the average velocity at a lower level has a greater value, the decreasing slopes of the lines are almost identical between the three middle positions. This implies that the mean velocity reducing rates are almost the same at different heights and slightly decrease as flow proceeds down the stream in the middle section of the room.

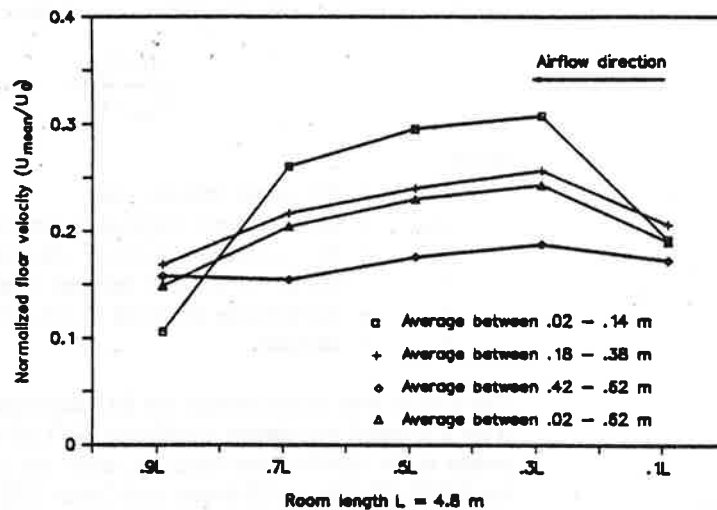


Fig. 6 The horizontal distributions of normalized time-mean velocity over different heights in the occupied zone.

Comparison with Common Jet Profile

Since the mean velocity distributions at the middle of the room have a similar form to a wall jet, further comparisons with wall-jet and free-jet profiles were conducted. Many empirical formulas expressing the normalized free-jet and wall-jet profiles have been developed. The most commonly used dimensionless form is

$$\frac{U}{U_{\max}} = \exp[-k(\frac{y}{y_{0.5}})^2] \quad (1)$$

where

- U/U_{\max} = the actual velocity normalized by the centerline or maximum velocity;
- $y/y_{0.5}$ = the non-dimensional length scale of actual distance from the centerline divided by the distance at which $U = 0.5U_{\max}$; and,
- k = an empirical constant. The k values were reported to be 0.698 [16], 0.696 [17] and 0.937 [18].

However, the velocities measured in this study were only taken up to 0.62 m from the floor. The velocity is still significant above this height. In order to exclude the velocities in the top region, a new form of equation was defined as

$$\frac{U - U_{\min}}{U_{\max} - U_{\min}} = \exp[-k(\frac{y}{y_{0.5}})^2] \quad (2)$$

where

- U = the actual velocity, m/s;
- U_{\max} = the maximum velocity in the profile, m/s;
- U_{\min} = the minimum velocity in the profile, m/s, U_{\min} should occur at $y = 0.62$ m;
- y = the actual distance between U and U_{\max} , m, $y = 0$ to 0.62 m;
- $y_{0.5}$ = the distance at which $U = 0.5(U_{\max} + U_{\min})$, m; and,
- k = constant.

The k value was found through the SAS non-linear least squares regression [14] to be 0.663 with a squared correlation coefficient (R^2) of 0.96. Figure 7 shows the actual measured points at the middle three room positions and the regression line. The k values suggested by ASHRAE [16] and Schwarz and Cosart [18] were also substituted into Equation 2 and the results are shown on the same figure. The present measurement is close to the result of Schwarz and Cosart [18] at low $y/y_{0.5}$ values and to that of ASHRAE [16] at high $y/y_{0.5}$ values. Although there is a difference between the definition of the formulas, the velocity profiles at the middle of the room do show, to a large extent, wall jet characteristics. However, Equation 2 may not be an appropriate expression for general use. When $U = U_{\min}$, y should be infinite; here y was only evaluated to 0.62 m above the floor.

Airflow at the Corner of the Occupied Zone

At the corners or the intersection of wall and floor, flow was restricted by the walls and the velocity direction of the main stream was deflected. Flow visualization showed that the main flow separated from the room interior surface at a certain separation point and started

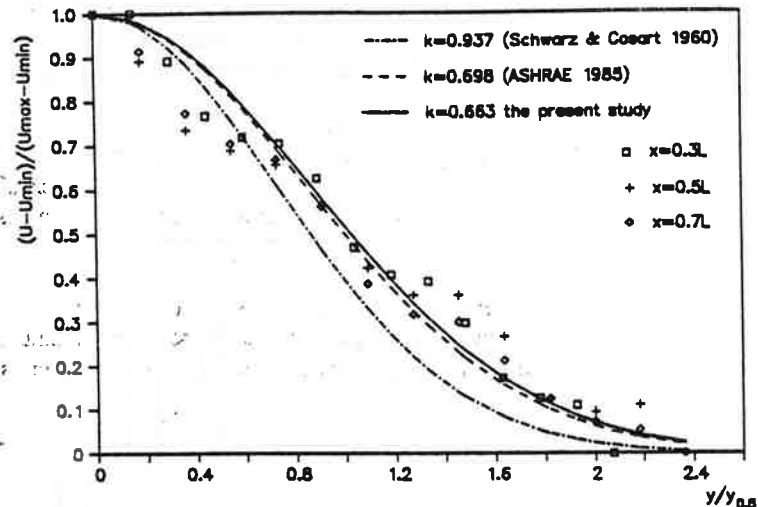


Fig. 7 The similar distributions of mean velocities at the mid-floor positions and the best fit regression line compared with common wall jet profiles.

to change flow direction as it approached a corner. The main part of the flow touched the adjacent surface of the same corner as it went along the deflected direction. One of the main streamlines was a boundary between the main flow and a "dead" region in the corner. Inside the small "dead" region, recirculation flows were formed causing high turbulence and vorticity. The magnitudes of the speeds and the area of the recirculating region at the corners were a function of the total energy contained by the flow and the energy expenditure during the flowing process. After the random interactions between flows, and losses of some energy at the corner, the main flow regained part of the energy and flowed in a new direction 90 degrees to its former direction. The averaged mean velocity profiles close to corners were less regular and smaller compared with those at the middle of the room shown on Figures 4, 5 and 6.

Turbulence Characteristics

The RMS value of the turbulent fluctuation components and the turbulence intensity, i.e. the ratio of RMS value to the mean velocity, are respectively the absolute and relative measures of the flow turbulence. Figures 8 and 9 respectively show the non-normalized and normalized averaged RMS values distributed vertically and Figure 10 shows the distribution horizontally. The low RMS values were found very near the floor starting from $x = 0.3L$ where the boundary layer of main flow stream began to form and the viscous effect on the fluid was relatively significant. As expected, the high RMS values occurred at the corners

and the upper or outer layer of the flow. The profiles from two individual inlet conditions are also shown on Figures 8 and 9 for comparisons. The magnitude of the RMS value was consistent with the mean velocity in Figures 4 and 5 and was different for the same ventilation flow rate. Therefore, it is not a single function of Q alone.

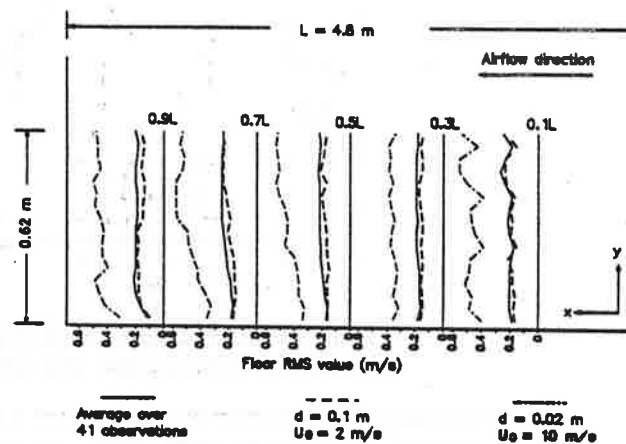


Fig. 8 The vertical distributions of non-normalized RMS values at five floor positions for overall 41 inlet conditions and the two typical settings.

Figure 11 shows the averaged turbulence intensities at 5 x positions. The horizontal distributions of at different levels above the floor is show on Figure 12. The small values occurred close to the floor in the middle three x positions and the large ones were at up flow region and the corners. The maximum averaged turbulence intensity was less than 50%. Comparing with Figures 4 or 5 and 6, the distributions the turbulence intensity were very like the mirror images of the mean velocity. Since turbulence intensity is a ratio of the RMS value to the mean velocity, it should be high when the mean is low if the RMS is relatively constant.

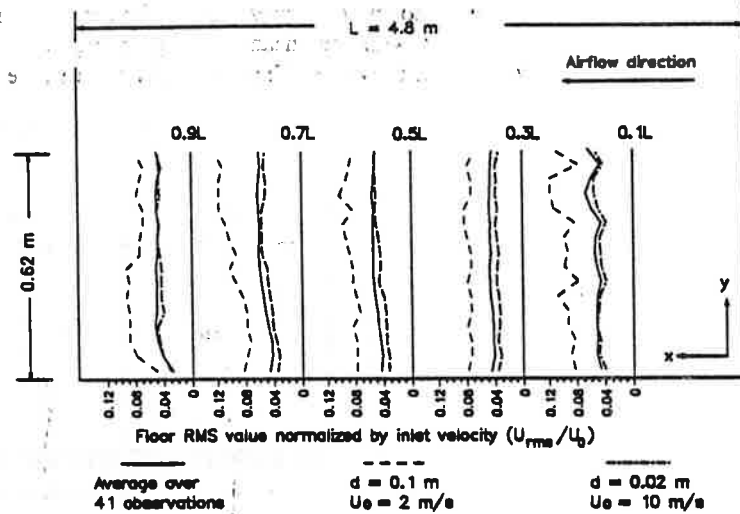


Fig. 9 The vertical distributions of normalized RMS values at five floor positions for overall 41 inlet conditions and the two typical settings.

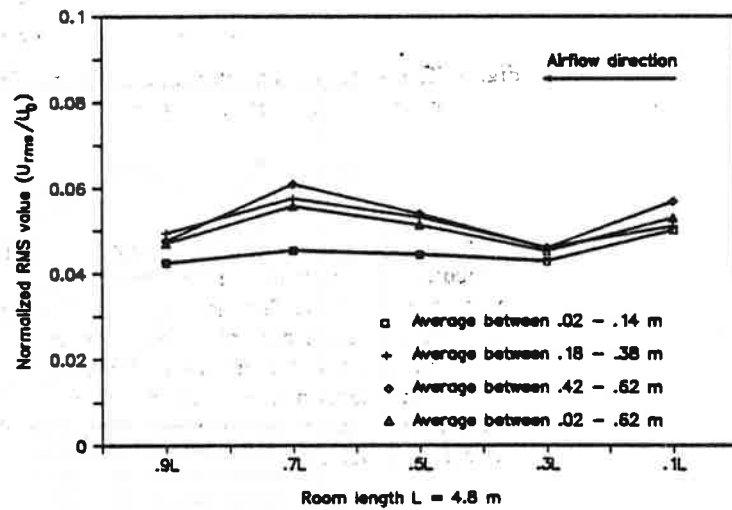


Fig. 10

The horizontal distributions of normalized RMS values over different heights in the occupied zone.

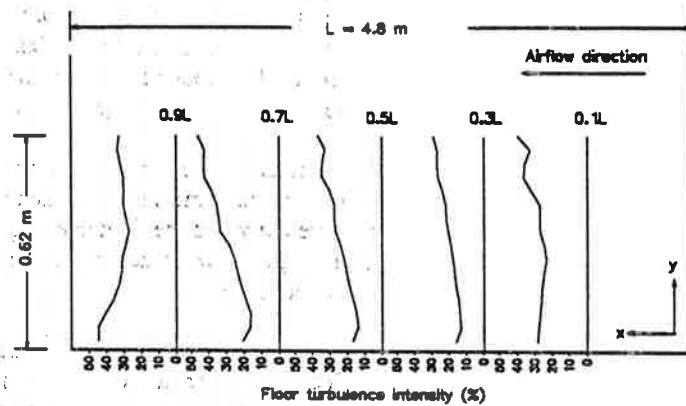


Fig. 11

The vertical distributions of the averaged turbulence intensity at five horizontal positions in the occupied zone.

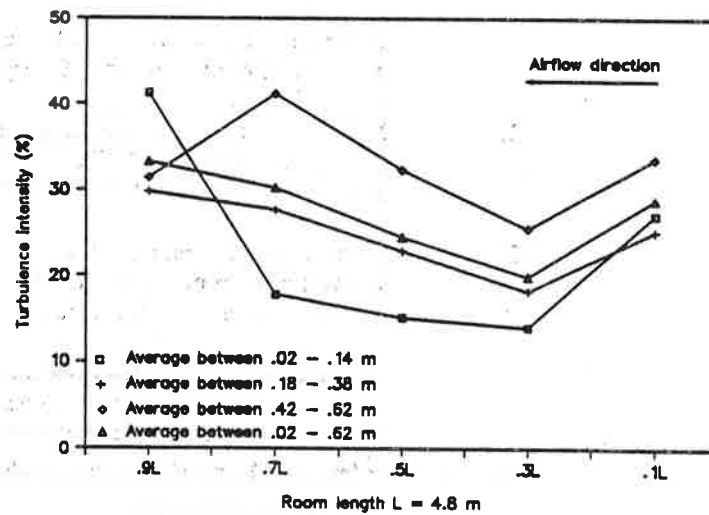


Fig. 12

The horizontal distributions of turbulence intensity over different heights in the occupied zone.

CONCLUSIONS

1. At middle of the floor region, the vertical distribution of the mean velocity had a similar form to and approximated a wall jet profile. The maximum velocity was found at 0.3 room lengths from the wall opposite to the inlet and at about 0.1 m above the floor. The decay rates of the mean velocity were the same at the different heights as the airflow proceeded in the occupied zone.
2. The actual and normalized floor airspeeds were different for the same ventilation flow rates through the inlet due to the different combinations of the inlet velocity and the inlet opening height. Ventilation flow rate is inadequate as a single index to determine the mean velocity and the RMS value in the occupied zone.
3. At the corners, the main flow stream was restricted and the flow direction was deflected. The small recirculation flows were formed in the corners, causing less regular mean velocity and high turbulence intensity.

REFERENCES

- [1] Fanger, P.O.; Melikov, A.K.; Hanzawa, H.; and Ring, J. "Air turbulence and sensation of draught." *Energy and Buildings*, 1988, 12, 1, pp. 21-39.
- [2] Nielsen, P.V.; Restivo, A.; and Whitelaw, J.H. "The velocity characteristics of ventilated rooms." *Transactions of the ASME, Journal of Fluids Engineering*, 1978, 100, pp. 291-298.
- [3] Gosman A.D.; Nielsen, P.V.; Restivo, A.; and Whitelaw, J.H. "The flow properties of rooms with small ventilation openings." *Transactions of the ASME, Journal of Fluids Engineering*, 1980, 102, pp. 316-323.
- [4] Nielsen, P.V. "Numerical prediction of air distribution in room - status and potentials." *Building Systems: Room Air and Air Contaminant Distribution*, Atlanta: American Society of Heating, Refrigerating, and Air-Conditioning Engineers, Inc., 1989, pp. 31-38.

- [5] Skovgaard, M. and Nielsen, P.V. "Numerical prediction of air distribution in rooms with ventilation of the mixing type using the standard k, ϵ model." *Nordisk Indeklima - arbejdsmiljø og energikonference*, Copenhagen, August 1990.
- [6] Timmons, M.B.; Albright, L.D.; Furry, R.B.; and Torrance, K.E. "Experimental and numerical study of air movement in slot-ventilated enclosures." *ASHRAE Trans.*, 1980, 86, 1, pp. 221-239.
- [7] Timmons, M.B. "Use of physical models to predict the fluid motion in slot-ventilated livestock structures." *Transactions of the ASAE*, 1984, 27, pp. 502-507.
- [8] Hanzawa, H.; Melikow, A.K.; and Fanger, P.O. "Airflow characteristics in the occupied zone of ventilated spaces." *ASHRAE Trans.*, 1987, 93, 1, pp. 524-539.
- [9] Melikov, A.K.; Hanzawa, H.; and Fanger, P.O. "Airflow characteristics in the occupied zone of heated spaces without mechanical ventilation." *ASHRAE Trans.*, 1988, 94, 1, pp. 52-70.
- [10] Melikov, A.K.; Langkilde, G.; and Derbiszewski, B. "Airflow characteristics in the occupied zone of rooms with displacement ventilation." *ASHRAE Transactions*, 1990, 96, 1, pp. 555-563.
- [11] Ogilvie J.R. and Barber, E.M. "Jet momentum number: an index of air velocity at floor level." *Building Systems: Room Air and Air Contaminant Distribution*, Atlanta: American Society of Heating, Refrigerating, and Air-Conditioning Engineers, Inc., 1989, pp. 211-214.
- [12] Spitler, J.D.; Pedersen, C.O.; and Fisher, D.E. "Interior convective heat transfer in buildings with large ventilation flow rates." *ASHRAE Trans.*, 1991, 97, 1.
- [13] Jin Y.; and Ogilvie, J.R. "Isothermal airflow characteristics in a ventilated room with a slot inlet opening." *ASHRAE Trans.*, 1992, 98, 2.
- [14] SAS Institute Inc. *SAS/STAT user's guide*, Release 6.03 Ed. Cary, NC: SAS Institute Inc., 1988
- [15] Jin, Y. "Airflow characteristics in a ventilated enclosure with a slot inlet opening." Ph.D. dissertation. School of Engineering, University of Guelph, Ontario, 1991.

- [16] ASHRAE. 1985 *ASHRAE handbook - fundamentals*, Chapter 32 American Society of Heating, Refrigerating, and Air-Conditioning Engineers, Inc., Atlanta, GA, 1985.
- [17] Beltaos, S and Rajaramam, N. "Plane turbulent impinging jets". *Journal of Hydraulic Research*, 1973, 11(1):29-59.
- [18] Schwarz, W.H. and Coşart, W.P. "The two-dimensional turbulent wall-jet." *J. Fluid Mech.*, 1960, 10, pp. 481-495.

